

High-intensity coherent FIR radiation from sub-picosecond electron bunches¹

Pamela H. Kung, Hung-chi Lihn and Helmut Wiedemann
Applied Physics Department and Stanford Synchrotron Research Laboratory,
Stanford Linear Accelerator Center, Stanford University, CA 94309
David Bocek
Physics Department and Stanford Synchrotron Research Laboratory,
Stanford Linear Accelerator Center, Stanford University, CA 94309

ABSTRACT

A facility to generate high-intensity, ultra-short pulses of broad-band far-infrared radiation has been assembled and tested at Stanford.¹ The device uses sub-picosecond relativistic electron bunches to generate coherent radiation through transition or synchrotron radiation in the far-infrared (FIR) regime between millimeter waves and wavelengths of about $100\ \mu\text{m}$ and less. Experimental results show a peak radiation power of greater than $0.33\ \text{MW}$ within a micro-bunch and an average FIR radiation power of $4\ \text{mW}$. The average bunch length of 2856 micro-bunches within a $1\ \mu\text{sec}$ macro-pulse is estimated to be about $480\ \text{fsec}$. Simulations, experimental setup and results will be discussed.

1 INTRODUCTION

Relativistic particles emit incoherent radiation at all wavelengths limited by the parameters of the process involved and additional coherent radiation at wavelengths of the order of the bunch length and longer. The coherent radiation spectrum is the Fourier transform of the electron distribution and reaches therefore from microwaves to far-infrared radiation of wavelength as short as the bunch length. Since coherent radiation is proportional to the square of the number of particles per bunch, very intense radiation can be expected compared to, for example, ordinary synchrotron radiation where the intensity is only linearly proportional to the number of particles. FIR radiation generated by short electron bunches exceeds greatly that of conventional sources, is broad band, and is temporally and spatially coherent. Such coherent radiation has been predicted theoretically² and has been observed by several groups in the form of microwaves from electron bunches of a few psec duration generated in linear accelerators.^{3,4} In synchrotrons no such coherent radiation has been detected yet presumably because the bunch lengths tend to be of the order of cm and propagation of electromagnetic waves of such wavelength is suppressed by the metallic vacuum chamber.

¹This research has been funded through SSRL by the Department of Energy, Office of Basic Energy Sciences and Department of Energy contract, DE-AC03-76SF00515.

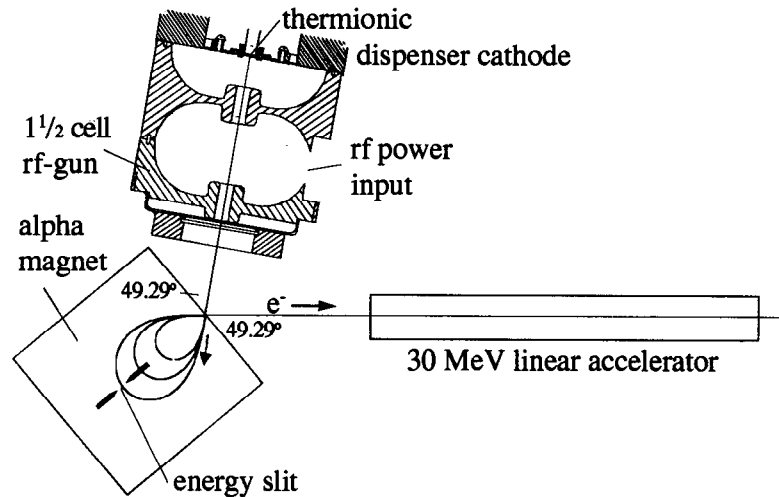


Figure 1: Rf-gun and bunch compression system

Table 1: Parameters for the FES experiment

energy	$E = 30$ MeV	e^- per micro pulse	$N_e \sim 4.6 \times 10^8$
	$\gamma = 58.7$	total electron flux	$\dot{N}_{e,tot} \geq 10^{12} e^-/sec$
pulse current	$I_p \leq 900$ mA	rf-pulse length	$T_{rf} = 1.5 \mu sec$
repetition rate	$R = 10$ pps	beam-pulse length	$T_b = 1 \mu sec$
micro-bunches/macro-pulse	$n_b = 2856$	bunch length	$\tau \geq 200$ fsec

The first step to generate intense coherent radiation is to produce very short intense electron bunches, which occupy only a very small area in phase space. A suitable source for such a beam is an rf-gun because space charge forces, which enlarge phase space area, are quickly overcome by rapid acceleration to relativistic energies of a few MeV. Appropriate rotation of the longitudinal phase space distribution in a magnetic compressor finally produces the desired short bunches. Presently compression of electron bunches is limited to the order of $100 \mu m$ and the obtainable radiation is therefore in the far-infrared regime. A facility to produce and study ultra-short electron pulses, the FES (Femtosecond Electron Source) has been assembled at Stanford consisting of a 2.5-MeV rf-gun, an alpha magnet with energy filter for bunch compression and a 30-MeV linear accelerator to produce femtosecond electron and photon pulses.¹ In Tab. 1 some design and expected performance parameters of the FES facility are compiled and Fig. 1 shows a schematic layout of the system.

2 CONCEPTUAL BACKGROUND

The method to produce ultra-short electron bunches is described in more detail in references^{1,5-7} and its main components are shown schematically in Fig. 1. An electron beam consisting of 2856 micro-bunches per μsec of rf pulse is generated at an energy of 2.5 MeV in an 1-1/2 cell rf-gun operated at 2856 MHz. Each micro-bunch is separated by 350 psec from the next one. The electrons in a micro-bunch occupy a very small area in phase space since the particle momentum is closely correlated to the time they emerge from the rf-gun. Fig. 2.a shows the results for the correlation of particle momentum and time from numerical simulations with the computer code

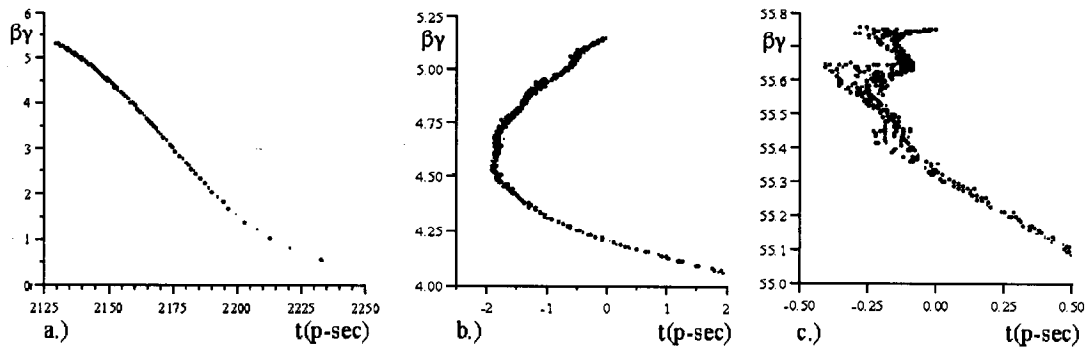


Figure 2: Particle momentum-time distribution a) at exit of rf-gun, b) after compression by the alpha magnet, and c) at the radiation source point.

MASK.⁸ The particles are distributed in phase space along a thin line occupying only a very small area. This feature can be exploited to produce beam pulses of very short duration by an appropriate rotation of the particle distribution in phase space.

The particle beam from the rf-gun is guided to a magnetic bunch compression system, which in our case is an alpha magnet,^{7,9} where particles of different momenta have different path lengths. The path in this magnet has the form of the Greek letter α and enters and exits at the same point for all momenta if the entrance angle with respect to the magnet axis is 49.29° (Fig. 1). The first particles in each micro-bunch coming from the rf-gun have high momenta and follow therefore longer paths in the alpha magnet while later particles with less momenta follow shorter paths. With the correct setting of the magnetic field it is possible to compress part of the rf-gun beam to extremely short bunches. Fig. 2.b shows the compressed particle distribution of Fig. 2.a after the alpha magnet. To select only the optimally compressed part of a micro-bunch a momentum selecting aperture is introduced into the alpha magnet filtering out the most compressed part of the original bunch.

Although the particles are relativistic, the velocity spread can cause a further spread of bunch length along the beam line which is significant on the scale of sub-picosecond bunches. The alpha magnet is therefore adjusted such that the electron bunch reaches the minimum bunch length not at the exit of the alpha magnet but rather at the source location of the FIR radiation. To achieve this the bunch must be overcompressed in the alpha magnet (Fig. 2.b). This produces a beam where the low energy particles are now ahead of the high energy particles, and this overcompression is compensated by the spread of velocities while being accelerated to 30 MeV in the linac and travelling along drift spaces. The degree of optimum overcompression or alpha magnet strength is determined by simulating the whole bunch motion from the rf-gun to the radiation source point. At 30 MeV the velocity spread is negligibly small in our case increasing the bunch duration only about 10 fsec per meter of drift length for a typical momentum spread of $\pm 0.5\%$.

In this experiment two methods of producing coherent FIR radiation have been investigated. In one method the electron beam passes through a thin Al-foil generating transition radiation.¹⁰ In the second method we observe coherent FIR synchrotron radiation from a bending magnet. Both will be described in more details later in Sec. 4.

The total radiated spectral power from a mono-energetic bunch of N_e electrons at wavelength λ is

$$P_{\text{tot}}(\lambda) = p(\lambda) N_e \left[1 + (N_e - 1) |g(\sigma_z, \lambda)|^2 \right], \quad (1)$$

where $p(\lambda)$ is the spectral radiation power from single electron and $g(\sigma_z, \lambda)$ is a form factor for an azimuthally symmetric bunch of length $2\sigma_z$, which is the Fourier transform of the actual particle distribution. The first term in the square bracket determines the incoherent part of the radiation while the second term describes the coherent

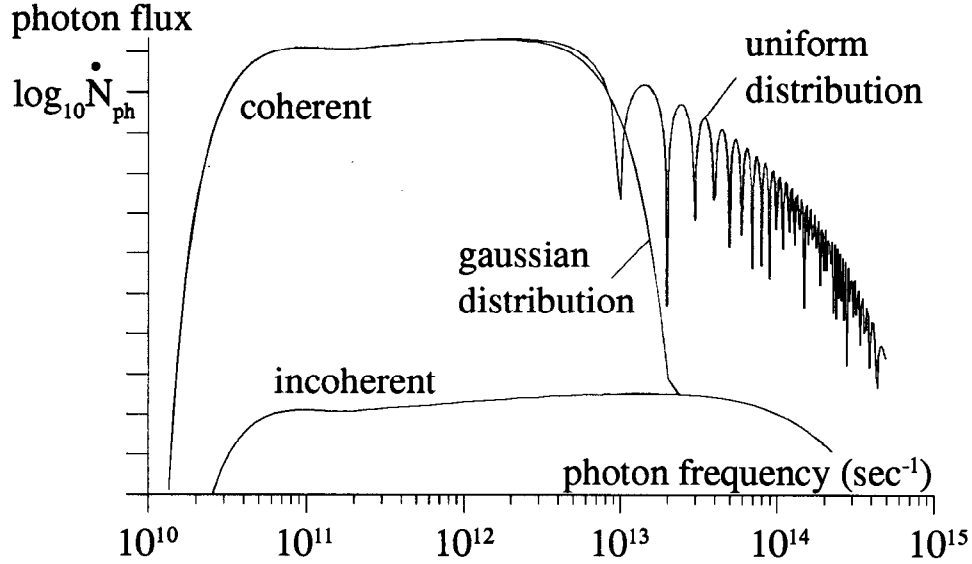


Figure 3: Coherent enhancement of synchrotron radiation

radiation. The form factor reduces to zero for wavelengths shorter than the bunch length and approaches unity for longer wavelengths. In particular

$$g(\sigma_z, \lambda) = \frac{\sin(2\pi\sigma_z/\lambda)}{2\pi\sigma_z/\lambda} \quad (2)$$

is the form factor for a rectangular particle distribution of width $2\sigma_z$ and

$$g(\sigma_z, \lambda) = \exp\left(-2\pi^2 \frac{\sigma_z^2}{\lambda^2}\right) \quad (3)$$

the form factor for a Gaussian distribution with standard deviation σ_z .¹¹

Whatever method to generate radiation is used, the coherent radiation intensity is greater than the incoherent radiation by a factor of $N_e |g(\sigma_z, \lambda)|^2$. Since N_e is generally very large it becomes possible to generate coherent FIR radiation of very high intensity. For example, the angular integrated spectral energy of transition radiation from a perfect conductor per electron is $d\epsilon/d\omega = 2r_c mc \ln \gamma/\pi$. Folding this with the form factor for a Gaussian distribution the average radiation power is approximately

$$P = \frac{r_c mc^2}{\sqrt{\pi}} n_b N_e^2 R \frac{\ln \gamma}{\sigma_z}, \quad (4)$$

where r_c is the classical electron radius. The maximum intensity of radiation is emitted into a rather small angle of $1/\gamma$. The high intensity emitted into a small solid angle from a small electron beam cross section results in a large value of the FIR source radiance at or approaching the diffraction limit.

Synchrotron radiation¹¹ is emitted over a characteristic spectrum. For short bunch radiation this spectrum is enhanced by $N_e |g(\sigma_z, \lambda)|^2$. The incoherent synchrotron radiation and coherent enhancement are shown in Fig. 3. The increased richness of harmonics for a uniform particle distribution compared to a Gaussian distribution is reflected in the high frequency extension of the radiation spectrum. The radiation is greatly collimated into the forward direction within an angle of $1/\gamma$ with respect to the beam axis.

3 NUMERICAL SIMULATION

The dynamics of electrons in the rf-gun is simulated with the help of the computer program MASK which includes space charge effects and produces therefore a selfconsistent solution. The simulation results in a distribution of many macro-particles in momentum and time as shown in Fig. 2. This distribution is then transformed by numerical integration to any point downstream from the rf-gun taking into account the spread in velocity as well as the compression in the alpha magnet and linac acceleration. The resultant distributions at the photon source points are then used to calculate the coherent radiation intensity. Space charge and emittance effect are neglected in this longitudinal transformation because both effects are small outside the rf-gun.

The fast oscillating rf-field together with a thermionic cathode produces an electron bunch with varying momenta from a maximum value to almost zero accompanied by a long tail in time. Fig. 2.a shows the longitudinal phase space distribution of particles in a single micro-bunch. Most particles are concentrated close to the maximum momentum with about 50-60% of all electrons actually being within a $\pm 10\%$ momentum spread and a time interval of about 13 psec at the exit of the gun. Performing numerical simulations under conditions expected during the experiment with parameters listed in Tab.1, we consider a beam pulse of $1 \mu\text{sec}$ duration consisting of a train of 2856 micro-bunches of equal intensity and equal bunch length of 200 fsec. Further we assume that the angular acceptance of the light collecting optics is 40 mrad for synchrotron radiation about the beam axis. Under such conditions the simulations¹² predict a total radiated energy of

$$1400 \mu\text{J per macro-pulse} \quad \text{for synchrotron radiation} \quad (5)$$

from a 2.2 kG dipole field and a beam intensity of 4.6×10^8 electrons per micro-bunch.

To calculate the intensity of transition radiation, we use more realistic formulae in reference¹³ which give the angular spectral density of transition radiation from a dielectric plate with an arbitrary incident angle. Substituting in the thickness of Al-foil ($25.4 \mu\text{m}$) and using Drude model for complex dielectric constant of Al,¹⁴ we get total radiation energy of

$$4192 \mu\text{J per macro-pulse} \quad \text{for transition radiation}$$

from a train of 2856 micro-bunches with equal bunch length of 200 fsec and equal intensity of 3.08×10^8 electrons per micro-bunch. If we further consider the finite acceptance of the observation window, only 36% of total radiation will be collected through the window, and this reduces the expected radiation energy down to

$$1514 \mu\text{J per macro-pulse} \quad \text{for transition radiation.} \quad (6)$$

In Sec. 5 we will compare these expected results with those measured ones.

4 EXPERIMENTAL SETUP

The FES facility is composed of two parts: along the first part the particle beam from the rf-gun is compressed in the alpha magnet and then accelerated to 30 MeV in a linear accelerator. An 1-1/2 cell rf gun⁵⁻⁷ with a thermionic cathode produces an electron beam at a momentum of about 2.5 MeV/c. The layout of the rf-gun and compression system is shown schematically in Fig. 1. The alpha magnet serves as a compressor for the electron bunches. The independently controllable aperture slits inside the alpha magnet can be used to select the desired energy bin or to control the electron current entering the linac. By choosing the field and slit positions of the alpha magnet, the shortest bunch is selected while discarding useless electrons.

The second part of the facility includes the radiation sources and the particle beam dump and is shown schematically in Fig. 4. Transition radiation is produced from a thin Al-foil installed on a retractable actuator

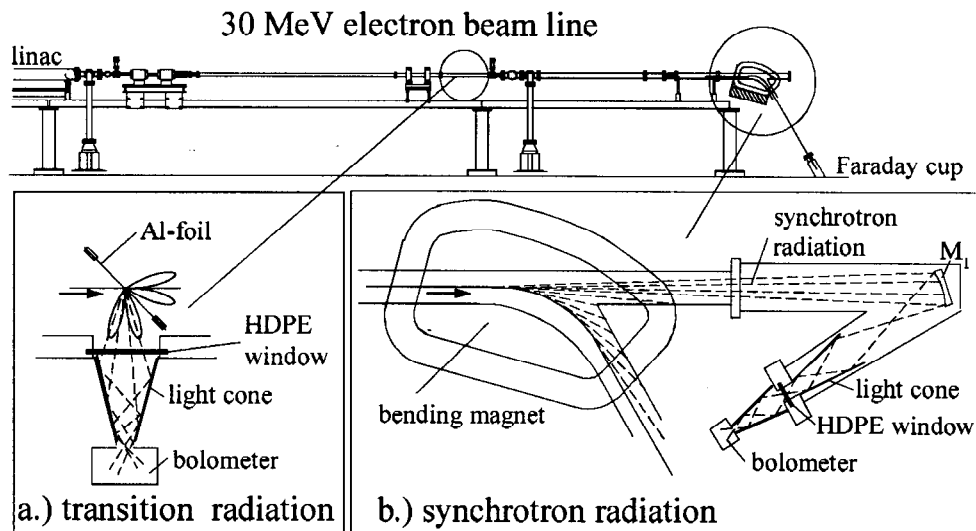


Figure 4: Electron beam line and radiation source points

(Fig. 4.a). Further downstream a dipole magnet which is used to deflect the electron beam to a Faraday cup is also used as the source of coherent synchrotron radiation (Fig. 4.b).

Transition radiation is generated while the electron beam is passing through a $25.4\text{-}\mu\text{m}$ -thick aluminum foil of 20 mm in diameter shown in Fig. 4.a. The foil supported by a copper ring is oriented at a 45° angle to the beam direction. A room-temperature pyroelectric bolometer collects the backward radiation at right angle to the electron beam direction through a 1.25-mm-thick high-density polyethylene(HDPE) window of 19 mm diameter and 87% transmission. The downstream side of the Al-foil was coated with zinc sulfide(ZnS) to monitor and optimize the electron beam size as well as its position.

Synchrotron radiation is collected by a 100-mm-diameter spherical mirror M1, 1.3 m away from the source point as shown in Fig. 4b, and deflects the focussed beam toward a 19-mm-diameter and 1.25-mm-thick HDPE window. The angular acceptance for the radiation is 40 mrad limited by the mirror diameter. A copper condensing cone¹⁵ channels the radiation through the HDPE window. The radiation originates from the fringe and main field of the dipole magnet and sweeps downward across the mirror M1. This arrangement is less than ideal and elaborate calculations to determine the collection efficiency are necessary.

The room-temperature bolometer consists of a Molecron LiTaO_3 pyroelectric detector and a pre-amplifier. Its sensitivity is uniform over a spectral range from visible light to millimeter waves covering the full range of expected coherent radiation. The electronic bandwidth of the detector can be selected from 20 Hz up to 70 MHz by an appropriate external resistor. The electronic bandwidth was set to around 20 Hz to integrate the radiated energy within a single macro-pulse without any interference with the adjacent macro-pulses. The electronic noise from fast switching devices in the linac modulator were kept below $100\ \mu\text{V}$ while the bolometer signal from coherent radiation was of the order of 0.3 V. Note that the bolometer voltages quoted in this paper have been taken away any pre-amplification. The bolometer has been calibrated against a Scientech thermopile power meter, which itself was absolutely calibrated by known electrical currents, and this gives the energy responsivity of $1.21 \times 10^8\ \text{V/J}$ for the pyroelectric detector. Since the diameter of the detector is only 5 mm, a light collecting copper cone is installed between the HDPE window and the bolometer to direct all radiation to the detector surface. A pulse transformer surrounding an isolated section of the beam pipe was used to measure the current distribution during the macro-pulse. No means was available to resolve individual micro-bunches.

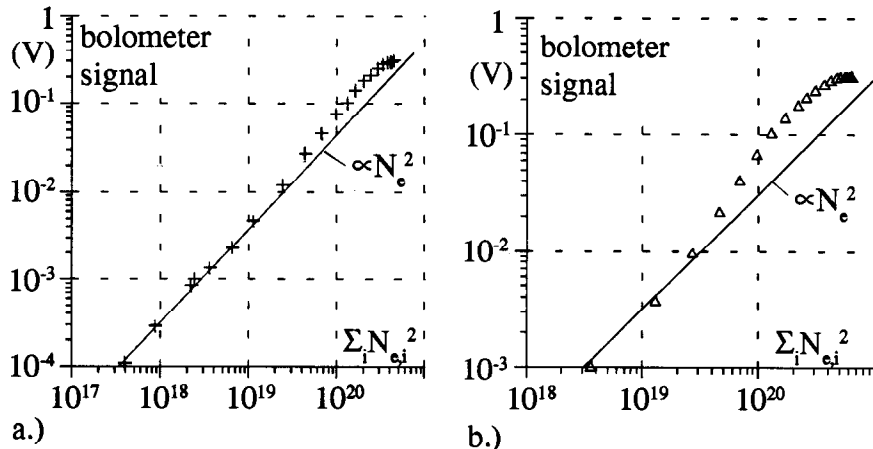


Figure 5: Scaling of a) coherent synchrotron radiation and b) coherent transition radiation signal (in Volts) with the square of number of particles per micro-bunch.

5 RESULTS AND DISCUSSION

Theoretically one expects the coherent radiation intensity to scale with the square of the number of particles N_e per micro-bunch. To vary the beam current we could not use the cathode heating current in the rf-gun because this would greatly affect the momentum distribution of the particles due to beam loading and lead to different compression in the alpha magnet. A neutral way to reduce beam current would be to use mechanical scrapers along the beam line, which however were not available. The most sensible way to vary the particle intensity available was to move the high energy aperture in the alpha magnet into the beam to scrape off some of it while keeping the low energy aperture constant. Since we intend to compress most of the high energy particles into a short bunch this method seemed to have the least effect on the bunch length.

The total radiation signal was measured with the bolometer as a function of the number of electrons derived from a fast current transformer at the exit of linac. Since the current pulse is nonuniform the transformer signal was dissected numerically into slices in time for each i^{th} slice of which the square of the number of particles, $N_{e,i}^2$, was calculated. In Fig. 5.a and Fig. 5.b the results are shown in log-log scale plotting the radiation signal as a function of the sum of squares of the particle numbers in each slice, $\Sigma_i N_{e,i}^2$, for the transition and synchrotron radiation, respectively.

Both measurements show the expected linear dependence over two to three orders of magnitude for both transition and synchrotron radiation. Small deviations from the ideal scaling are due to unavoidable variations of the effective bunch length for different segments of the momentum spectrum selected by this method. No part of the measurements indicates that the radiation was from regular incoherent radiation, which is theoretically more than eight orders of magnitude less intense.

There are, however, other possible sources of radiation such as ionizing particle radiation hitting directly the bolometer or wake field radiation. To eliminate the possibility that the detector signal comes from direct particle radiation a vacuum valve between the electron beam and the light collecting mirror M1 was closed upon which the bolometer signal was reduced from 0.3 V to less than 100 μ V. Since the vacuum valve did not obstruct direct line of sight from the particle beam to the bolometer we exclude the possibility that the measured signal originated from ionizing radiation. In a more direct measurement the electron beam was aimed into the stainless steel vacuum chamber close to the detector generating a signal of only a few hundred μ V.

Wake field radiation occurs in the form of cm and mm microwaves and is well known in accelerator physics where high charge densities occur. Such radiation originates from the electromagnetic interaction of the particle beam with its surroundings, specifically sudden changes in the cross section of the vacuum chamber. The radiation loss can be estimated from known impedances for typical vacuum chamber components and is of the order of nJ for the beam parameters used here compared to an observed radiation energy of 200–400 μJ . We therefore exclude the possibility that the observed bolometer signal was caused by wake field radiation. Much of such wake field radiation would be expected to come from the linac structure. By steering the electron beam emerging from the linac transversely away from the transition radiator, the bolometer signal reduced below the electronic noise level although wake field would still be able to reach the Al-foil. This again rules out the possibility of wake field radiation.

A total radiation energy from all bunches in a macro-pulse of

$$262 \mu\text{J per macro-pulse} \quad \text{for synchrotron radiation} \quad (7)$$

with an rms micro-bunch particle intensity of 4.6×10^8 electrons and

$$382 \mu\text{J per macro-pulse} \quad \text{for transition radiation} \quad (8)$$

with an rms micro-bunch particle intensity of 3.08×10^8 electrons has been measured. This is obviously significantly below the expected intensity (Eqs. 5 and 6) from simulations discussed in Sec. 3. A number of correction to simulations as well as measured values must be applied. In both cases the measured radiation intensity should be corrected for the 87% transmission efficiency of the HDPE window while other corrections are specific to synchrotron or transition radiation.

The collection efficiency of synchrotron radiation depends on several factors. Firstly as the electrons bend in the dipole magnet, the emitted radiation changes direction and moves off the spherical mirror(M1). Secondly as the electrons enter the dipole magnet, the magnetic field increases from zero to its nominal value. We model this fringe field as a linear variation from zero up to the nominal value over a distance equivalent to one pole gap of 40 mm. This fringe field contributes to the observed radiation and cannot be ignored. Thirdly the power and opening angle of radiation at a particular wavelength is a function of electron beam energy and magnetic field. The opening angle can be expressed for our situation approximately by¹¹

$$\sigma_{\theta} \text{ (mrad)} = \frac{7.124}{[\rho \text{ (m)} E_{\text{photon}} \text{ (eV)}]^{1/3}} \quad (9)$$

Finally, not all the radiation intercepted by M1 passes through the condensing cones. Ray tracing in the axial plane of the cones was used to find their angular acceptance.

Taking into account the above factors, the amount of collected energy is then the sum of all contributions along the beam trajectory in the dipole magnet. This energy is normalized to the simulated radiation energy under ideal conditions as described in Sec. 3 to determine the collection efficiency. In the experimental setup used this collection efficiency varies from 35% for radiation from a bunch length of 1.25 psec to 62% for that of 0.15 psec.

Furthermore we note that the simulation assuming the same bunch length for all micro-bunches within a macro-pulse does not correctly resemble the actual situation. The momentum distribution during a macro-pulse has been measured using the energy slits in the alpha magnet and is shown in Fig. 6 in form of a spectral plot. The horizontal axis is the time and the vertical axis the momentum with a resolution $\Delta(\beta\gamma)$ of 0.05. Different shades represent levels of beam current. The change in the central momentum, which has the highest beam intensity at a given time, throughout a macro-pulse resembles different rf-field levels in the rf-gun at different times due to varying beam loading. This variation converts into a time varying bunch length for a constant setting of the alpha magnet. Simulations show that the bunch lengths for the different momenta during the macro-pulse vary from 1.2 psec down to 0.2 psec for rf fields different by only a few percent for the constant alpha magnet strength.

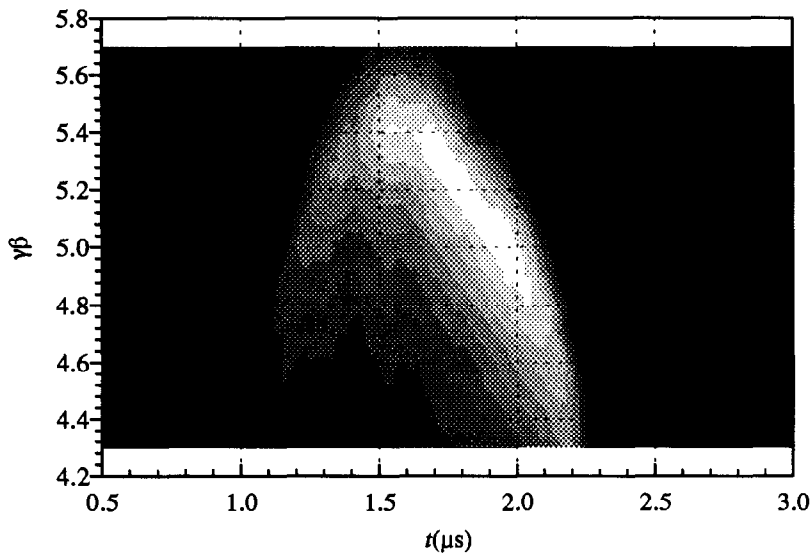


Figure 6: Spectral plot of particle distribution in a macro-pulse from an rf-gun

In a revised simulation the macro-pulse was dissected into short slices in time. The micro-bunch length and bolometer signal are then calculated based on the measurement of the momentum and current in each slice. Summation of all radiated energies from each segment of the macro-pulse gives a new simulated total radiation energy of

$$479 \text{ } \mu\text{J per macro-pulse} \quad \text{for synchrotron radiation} \quad (10)$$

and

$$560 \text{ } \mu\text{J per macro-pulse} \quad \text{for transition radiation.} \quad (11)$$

The variation of the micro-bunch length within the macro-pulse has obviously greatly reduced the total and spectral radiation obtainable. This total synchrotron radiation power is equivalent to that from 2856 micro-bunches with equal bunch length of 475 fsec and equal intensity of 4.6×10^8 electrons, while the total transition radiation power is equivalent to that with equal bunch length of 483 fsec and equal intensity of 3.08×10^8 electrons.

To summarize, we collect the results of simulations and measurements with corrections discussed above and obtain for synchrotron radiation:

simulated radiation signal	479 μJ ,
include collection efficiency (52%)	249 μJ ,
include window loss	217 μJ ;
measurement	262 μJ .

For the case of synchrotron radiation we have achieved agreement between simulations and measurements to within 10%. Some of the excess radiation measured compared to simulations may very well come from synchrotron radiation generated by beam steering fields along the beam line. Similarly we get for transition radiation:

simulated radiation signal	560 μJ ,
include window loss	487 μJ ;
measurement	382 μJ .

Again the agreement between simulation and measurement is close and may be even closer after including corrections for a not quite ideal light collecting cone.

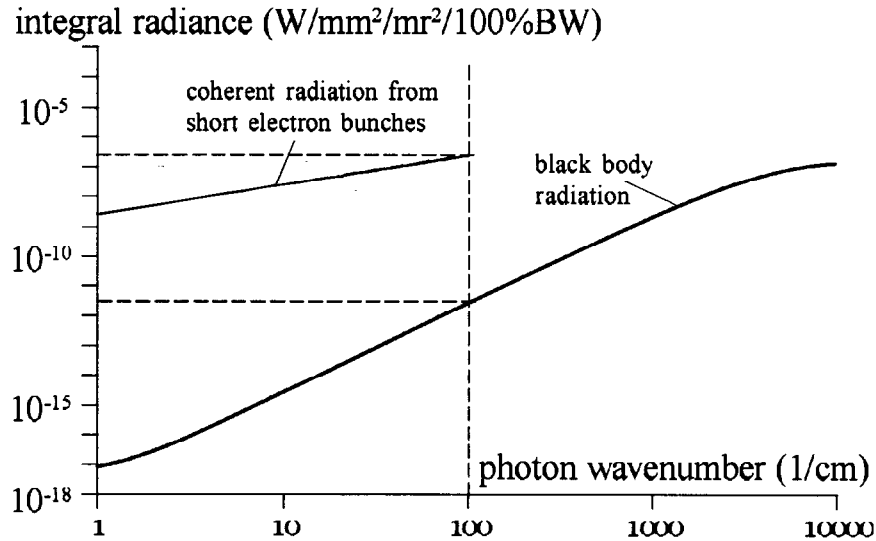


Figure 7: Comparison of the integral FES radiance(in $W/mm^2/mrad^2/100\%BW$) with black body radiation

6 CONCLUSION

It has been demonstrated in this experiment that intense relativistic electron bunches can be compressed longitudinally to less than 480 fsec or about $140 \mu m$. Such electron bunches radiate collectively and produce coherent far-infrared radiation of high radiance exceeding conventional black body sources by more than five orders of magnitude. In Fig. 7 we compare the integral radiance of the FES with that of an ideal black body radiator at 2000 K.

For the black body radiation it was assumed that all radiation emerges from a $10 mm^2$ source and Fig. 7 shows the integral radiance for all wavenumbers up to the value k . In the absence of spectral measurements it was assumed that the short bunch radiation is emitted into a flat spectrum up to a wavenumber of $100 cm^{-1}$ or down to a wavelength of $100 \mu m$. The radiation was assumed to emerge from an electron beam with a diameter of 2 mm into the full angular acceptance of the light collecting optics of 40 mrad about the beam axis. No diffraction effects have been included. The radiance was then adjusted such that the total radiation energy for wavelengths of $100 \mu m$ and longer was equal to the total measured radiation energy of $400 \mu J$ per macro-pulse. Under these assumptions the far-infrared radiation source described here is up to five orders of magnitude brighter than conventional sources. Spectral measurements are in preparation to obtain a more accurate comparison. The radiation covers a broad spectrum determined by the Fourier transform of the electron micro-pulse.

Numerical simulation of bunch compression and production of radiation agree quantitatively with measurements and can be used to optimize the radiation source further. Also further studies are required to produce a more uniform beam.

7 FUTURE DEVELOPMENTS

In this paper, we have shown that the measurements based on the collective results of 2856 different micro-bunches. To further study the detailed bunch structure of this varying macro-pulse, a similar type of bolometer

with faster electronic response up to several MHz is being built. A FIR Michelson interferometer is also under construction, which can be used to study the optical spectrum of this high power source.

In addition to broad-band high power FIR radiation, one can also use periodic photon generating devices to enhance the the coherent radiation at a certain wave length, hence, generate narrow-band high power FIR radiation. For example, an undulator is currently being constructed and tested at FES to perform this function. This would make FES a more versatile light source.

8 ACKNOWLEDGEMENT

The authors would like to thank for the engineering and mechanical support by M. Baltay, C. Chavis, D. Day, J. Haydon, G. Husak, R. Ornelas, J. Sebek, and K. Zuo during the construction period of the FES facility.

9 REFERENCES

- [1] H. Wiedemann, P. Kung, H.C. Lihn, "Ultra-short electron and photon pulses," Nucl. Instr. and Meth., A319, pp. 1-7, 1992.
- [2] F. Michel, Phys. "Intense coherent submillimeter radiation in electron storage rings," Phys. Rev. Let., Vol. 48, pp. 580-583, 1982.
- [3] T. Nakazato et.al., "Observation of coherent synchrotron radiation," Phys, Rev. Let., Vol. 63, No. 12, pp. 1245-1248, 1989.
- [4] E. B. Blum, U. Happek, A.J. Sievers, "Observation of coherent synchrotron radiation at the Cornell linac," Nucl. Instr. and Meth., A307, pp. 568-576, 1991.
- [5] E. Tanabe, et. al. "A 2-MeV microwave thermionic gun," *Proc. of the 14th Meeting on Linear Accelerators*, Nara, Japan, September 1989.
- [6] M. Borland et. al., "Performance of the 2-MeV microwave gun for the SSRL 150-MeV linac," *Proc. of the Linear Accel. Conf*, Albuquerque, Sept. 1990.
- [7] M. Borland, *A High-brightness Thermionic Microwave Electron Gun*, PhD Thesis, Stanford University, April 1991.
- [8] A. T. Drobot et. al., "Numerical simulation of high power microwave sources," IEEE Trans. Nucl. Sci., Vol. NS-32, No. 5, pp. 2733-2737, 1985.
- [9] H. A. Enge, "Achromatic magnet mirror for ion beams," Rev. Sci. Instr., Vol. 34, No. 4, pp. 385-389, 1963.
- [10] U. Happek, A.J. Sievers and E.B. Blum, "Observation of coherent transition radiation," Phys. Rev. Let., Vol. 67, No. 21, pp. 2982-2965, 1991.
- [11] H. Wiedemann, *Particle Accelerator Physics*, Springer Verlag, Heidelberg 1993.
- [12] H. C. Lihn, "Simulation of coherent synchrotron radiation from an ultra-short electron bunch," SSRL ACD Note 124, Stanford, 1992.
- [13] M.L. Ter-Mikaelian, *High-Energy Electromagnetic Process in Condensed Media*, Wiley & Sons, pp. 219-220, New York, 1972.
- [14] D. Y. Smith, E. Shiles and M. Inokuti, "The optical properties of metallic aluminum," *Handbook of Optical Constants of Solids*, E.D. Palik ed., pp. 369-406, Academic Press Inc., 1985.

[15] D. Williamson, "Cone channel condenser optics," J. Opt. Soc. Am., Vol. 42, pp. 712-715, 1952.